**A&A manuscript no.**
(will be inserted by hand later)

**Your thesaurus codes are:**
**12.04.1 - 10.08.1 - 10.19.3 - 08.12.2**

ASTRONOMY AND ASTROPHYSICS

# Microlensing towards different Galactic targets

**Lukas Grenacher**[1,2]**, Philippe Jetzer**[1,2]**, Marcus Strässle**[2] **and Francesco De Paolis**[3]

[1] Paul Scherrer Institut, Laboratory for Astrophysics, CH-5232 Villigen PSI
[2] Institut für Theoretische Physik der Universität Zürich, Winterthurerstrasse 190, CH-8057 Zürich, Switzerland
[3] Department of Physics and INFN, University of Lecce, CP 193, I-73000 Lecce, Italy

Received; accepted



**Abstract.** We calculate the optical depth and the number of events due to gravitational microlensing towards the Galactic bulge, the spiral arm directions $\gamma$ Scutum, $\beta$ Scutum, $\gamma$ Normae, $\vartheta$ Muscae and some dwarf galaxies in the halo of the Galaxy.

Using the events found by the MACHO collaboration during their first year of observation towards Baade's Window we estimate the mass functions for the bulge and disk populations following the mass moment method. We find that the mass function can be described by a decreasing power-law with slope $\alpha \simeq 2.0$ in both cases and a minimal mass of $\sim 0.01\ M_\odot$ for the bulge and $\sim 0.02\ M_\odot$ for the disk, respectively. Assuming that the obtained mass function for the disk is also valid in the spiral arms, we find that the expected number of events towards the spiral arms is in reasonable agreement with the observations. However, the small number of observed events does not yet constrain much the different parameters entering in the computation of the mass function.

To study the influence of the Magellanic Clouds on the shape and the velocity dispersion in the halo we perform a N-body simulation. We find that their presence induces a slight flattening of the halo ($q_H \simeq 0.8$). As a result the expected number of microlensing events towards some targets in the halo, such as the LMC or the SMC, decreases by about 20%, whereas due to the the modification induced on the velocity dispersion the event duration increases.

**Key words:** dark matter - Galaxy: stellar content, structure - microlensing - stars: low-mass, brown dwarfs

## 1. Introduction

During the last ten years amazing progress was made by exploring the dark component of our own Galaxy by means of gravitational microlensing, as proposed by Paczyński in 1986. Microlensing allows the detection of MACHOs (Massive Astrophysical Compact Halo Objects) in the mass range $10^{-7} \lesssim M/M_\odot \lesssim 1$ (De Rújula et al. 1992) located in the Galactic halo, as well as in the disk or bulge of our Galaxy (Pazcyński 1991, Griest et al. 1991). Microlensing searches have nowadays become an important branch in astrophysics, especially for the study of the structure of the Milky Way and even for globular clusters (Jetzer et al. 1998).

Today, more than half a dozen groups are active in observing microlensing events towards different lines of sight, and they reported so far several hundreds of events, most of them towards the Galactic bulge (Alcock et al. 1997a, Udalski et al. 1994, Alard et al. 1997), some towards the spiral arms (Alcock et al. 1997a, Derue et al. 1999), about 15 events towards the LMC (Alcock et al. 1993, 1997b, Auburg et al. 1993) and two events towards the SMC (Alcock et al. 1997c, Palanque-Delabrouille et al. 1997, Udalski et al. 1997). The necessity to extend the microlensing target regions, as for instance towards M31 (Crotts & Tomaney 1996, Ansari et al. 1999), is widely recognized in order to better characterize the MACHO distribution throughout the Milky Way and the Galactic halo.

In this paper we calculate the optical depth and the number of events due to gravitational microlensing towards the bulge, the spiral arm directions $\gamma$ Sct, $\beta$ Sct, $\gamma$ Nor, $\vartheta$ Mus and some dwarf galaxies in the halo of the Galaxy. To that purpose we use the method of mass and time moments (De Rújula, Jetzer and Massó 1991). Based on a model of our Galaxy and taking into account the different populations of objects that can act either as lenses or as sources in microlensing events, we compute the different mass and time moments, which are needed for the determination of the various microlensing quantities. Due to the extension of the bulge we include in the calculation of the optical depth and the expected number of events the fact that the number density of sources varies with distance.

The 41 events published by the MACHO collaboration towards Baade's Window allow us to calculate the mass functions for the objects acting as lenses towards the Galactic bulge. The result is described by a decreasing power-law with $M_{min} \simeq 0.012 M_\odot$ for lenses in the bulge and $M_{min} \simeq 0.021 M_\odot$ for lenses in the disk and a slope $\alpha \simeq 2.0$ in both cases. Moreover, assuming that the disk mass function is the same also in the spiral arms, we find that the calculated number of events towards the spiral arms is in good agreement with the events reported by the EROS II collaboration.

*Send offprint requests to*: lugre@physik.unizh.ch

However, the small number of observed events towards the spiral arms does not yet constrain much the different parameters of the mass function.

We emphasize that, due to the small number of events at disposal, the mass functions we found for the bulge and the disk should be considered as an illustrative example of how the mass moment method can be used to get useful information on the physical parameters. Indeed, when the many new events which have been observed in the meantime will be published, more accurate results will be obtained.

To study the influence of the Magellanic Clouds on the shape and the velocity dispersion in the halo we perform a N-body simulation. We find that their presence induces a slight flattening of the halo ($q_H \simeq 0.8$) starting from an initially isotropic distribution. As a result the expected number and the duration of microlensing events towards targets in the halo gets modified.

The paper is organized as follows: in Sect. 2 we present our Galaxy model, in Sect. 3 we introduce the method of mass and time moments. The calculation of the various microlensing quantities towards the Galactic center and the spiral arms is done in Sect. 4, while Sect. 5 is dedicated to different targets in the halo of the Galaxy. A short discussion in Sect. 6 concludes the paper. The N-body simulation of the Galactic halo is presented in the Appendix.

## 2. Galaxy models

Our Galaxy model consists of three components: a bulge, a disk and a halo, which we discuss in the following.

### *2.1. Mass density*

Following Han and Gould (1995) we assume a triaxial bulge with a density law (Dwek et al. 1995) [1]

$$\rho_B(x', y', z') = \rho_{\circ B}\, e^{-s^2/2} = \frac{M_B}{6.57\pi abc}\, e^{-s^2/2}\,, \qquad (1)$$

with $s^4 = \left(x'^2/a^2 + y'^2/b^2\right)^2 + z'^4/c^4$. $M_B \simeq 1.8\times10^{10}\, M_\odot$ is the estimated bulge mass. The length scales are: $a = 1.58$ kpc, $b = 0.62$ kpc and $c = 0.43$ kpc ($x'$ and $y'$ are defined along and perpendicular to the bar shaped bulge in the Galactic plane). We take for the inclination angle between the bar major axis and the line of sight towards the Galactic center a value of $\Phi_\circ = 20^\circ$. The influence of this parameter on the results will be discussed.

We consider a disk model with a thin and a thick component and a density distribution as given by Bahcall et al. (1983) and Gilmore et al. (1989)

$$\rho_D(R,z) = \frac{1}{2}\, \exp\left[-\frac{(R-R_0)}{h}\right] \times \left[\frac{\Sigma_{\rm thin}}{H_{\rm thin}} \exp\left(-\frac{|z|}{H_{\rm thin}}\right) + \frac{\Sigma_{\rm thick}}{H_{\rm thick}} \exp\left(-\frac{|z|}{H_{\rm thick}}\right)\right]\,, \qquad (2)$$

where $R$, $z$ are cylindrical coordinates. Here we adopt $H_{\rm thin} \simeq 0.3$ kpc for the thin and $H_{\rm thick} \simeq 1$ kpc for the thick disk component, whereas $h \simeq 3.5$ kpc for the length scale of the two disks. Following Gates et al. (1995), we take for the local surface densities $\Sigma_{\rm thin} \simeq 25\ M_\odot/{\rm pc}^2$ and $\Sigma_{\rm thick} \simeq 35\ M_\odot/{\rm pc}^2$. $R_0 = 8.5$ kpc is the distance of the solar system from the Galactic center.

The halo is assumed to be a self-gravitating isothermal sphere of an ideal gas in hydrostatic equilibrium. A slightly flattened halo can then be described by the density distribution

$$\rho_H(x,\, y,\, z) = \frac{\rho_{\circ H}}{q_H}\, \frac{R_c^2 + R_0^2}{R_c^2 + \dfrac{z^2}{q_H^2} + x^2 + y^2}\,, \qquad (3)$$

where $q_H$ is the axis oblateness ratio (Binney and Tremaine 1987), $R_c \simeq 5.6$ kpc is the core radius and $\rho_{\circ H} \simeq 7.9 \times 10^{-3}\ M_\odot\ {\rm pc}^{-3}$ is the local dark mass density.

For the mass within 50 kpc we obtain for the bulge $M_B = 1.8 \times 10^{10} M_\odot$, disk $M_D = 5.2 \times 10^{10} M_\odot$ and halo $M_H = 4.3 \times 10^{11} M_\odot$, respectively. Thus the total mass is $M_{\rm tot} \simeq 5 \times 10^{11} M_\odot$ in agreement with e.g. Kochanek (1995). The calculated rotation curve agrees well with the measured values.

### *2.2. Mass distribution*

The mass density does not determine the MACHO number density as a function of mass alone. Assuming the mass-distribution to be independent of the position in the galaxy, the number density can be written as

$$\left(\frac{dn}{d\mu}\right)_i d\mu = \left(\frac{dn_\circ}{d\mu}\right)_i \frac{\rho_i(\mathbf{r})}{\rho_{\circ_i}}\, d\mu\,, \qquad (4)$$

where $\mu$ is the MACHO mass in solar mass units. The subscript $i$ stands for the bulge (B), the disk (D) or the halo (H). The MACHO number density per unit of mass, $dn_\circ/d\mu$, is normalized as follows:

$$M_\odot \int_{\mu_{min}}^{\mu_{max}} \left(\frac{dn_\circ}{d\mu}\right)_i \mu d\mu = \rho_{\circ_i}\,. \qquad (5)$$

The total mass distribution is just the sum over the components in Eq.(4). We assume a maximal mass $\mu_{max} \simeq 10\, M_\odot$ for the stars. However, only the faint stars up to about $\mu_{up} \simeq 1\, M_\odot$ can contribute to microlensing events. For the bright stars $\mu \geq 1\, M_\odot$ we assume a Salpeter IMF ($dn_0/d\mu \propto \mu^{-2.35}$), whereas for the lenses we will either assume all objects to have the same mass $\mu_{\circ_i}$ and, therefore, the mass distribution is described by a delta function

$$\left(\frac{dn_\circ}{d\mu}\right)_i = \frac{\rho_{\circ_i}}{M_\odot \mu_{\circ_i}} \delta(\mu - \mu_{\circ_i}) \qquad (6)$$

or we assume a power-law

$$\left(\frac{dn_\circ}{d\mu}\right)_i = C_i^1(\alpha_i)\mu^{-\alpha_i}\,. \qquad (7)$$

[1] The integral $\int_{-\infty}^{\infty} \exp(-s^2/2) dx' dy' dz'$ evaluates to $6.57\pi abc$. In the literature sometimes the wrong normalization $1/(8\pi abc)$ is used instead.

Accordingly the factor $C_i^1(\alpha_i)$ in the power-law is fixed by the normalisation condition (for $i = B,\ D$)

$$\frac{\rho_{0_i}}{M_\odot} = C_i^1 \int_{\mu_{min}}^{\mu_{up}} \mu^{1-\alpha} d\mu + C_i^2 \int_{\mu_{up}}^{\mu_{max}} \mu^{1-2.35} d\mu \,. \tag{8}$$

Assuming continuity for the mass function at $\mu_{up} = 1\,M_\odot$ we get

$$C_i^1(\alpha_i) = \frac{\rho_{\odot_i}}{M_\odot} \begin{cases} \left[\frac{1-\mu_{min}^{2-\alpha_i}}{2-\alpha_i} + 1.5809\right]^{-1} & \text{if } \alpha_i \neq 2 \\ [-\ln \mu_{min} + 1.5809]^{-1} & \text{if } \alpha_i = 2. \end{cases} \tag{9}$$

### *2.3. Velocity distribution*

For sources and lenses located in the bulge we assume that the velocity distribution along the various axes is Gaussian $f(v_y, v_z) = f(v_y)f(v_z)$, where

$$f(v_y) = \frac{1}{\sqrt{2\pi}\sigma_y} \exp\left[-\frac{(\mathrm{v_y} - \bar{\mathrm{v}}_\mathrm{y})^2}{2\sigma_\mathrm{y}^2}\right] \tag{10}$$

and a corresponding distribution for $f(v_z)$. The mean velocities $\bar{v}_y$ and $\bar{v}_z$ are supposed to be zero and the dispersion velocities $\sigma_y$ and $\sigma_z$ are deduced from the tensor virial theorem (Binney & Tremaine 1987). Following Han & Gould (1995) the dispersion velocities in the coordinate system given by the principal axes of the bulge ellipsoid are $(\sigma_{x'}, \sigma_{y'}, \sigma_{z'}) = (113.6, 77.4, 66.3)$, where the mean line of sight dispersion velocity is normalized to 110 km s$^{-1}$. The projected velocity dispersions in Galactic coordinates (such that $x$ is along the line of sight, $x-y$ is in the Galactic plane and $z$ perpendicular to it) are then computed to be $(\sigma_x, \sigma_y, \sigma_z) = (110, 82.5, 66.3)$. In the following it is convenient to write the distribution function $f(v_y, v_z)$ introducing polar coordinates in the $v_y - v_z$ plane. This way in polar coordinates the transverse velocity distribution turns out to be

$$f_{T,B}(\nu, \vartheta) d\nu d\vartheta = \frac{\nu}{\pi}\, \mathrm{e}^{-\nu^2} \mathrm{d}\nu \mathrm{d}\vartheta \,. \tag{11}$$

The transverse velocity is then given by

$$v_T = \nu \sqrt{2(\sigma_y^2 \cos^2\vartheta + \sigma_z^2 \sin^2\vartheta)} \,. \tag{12}$$

$\vartheta$ is the polar angle and the variable $\nu$ is dimensionless.

In the halo we consider a Maxwellian velocity distribution with typical dispersion velocity of $v_H = \sqrt{2}\sigma_H \simeq 220$ km s$^{-1}$ (Paczyński 1991). The transverse velocity distribution is then given by

$$f_{T,H}(v_T) dv_T = \frac{2}{v_H^2} v_T \exp\left(\frac{-v_T^2}{v_H^2}\right) dv_T \,. \tag{13}$$

For lenses belonging to the disk, the velocities of the observer and the source transverse to the line of sight are $\mathbf{v}_0$ and $\mathbf{v}_s$, respectively, and the transverse velocity of the microlensing tube of radius $R_E$ (where the Einstein radius $R_E$ will be defined in Sect. 3) at position $xD$ ($0 \leq x \leq 1$) is $\mathbf{v}_t(x) = (1-x)\mathbf{v}_0 + x\mathbf{v}_s$. Its absolute value is

$$v_t(x) = \sqrt{(1-x)^2|\mathbf{v}_0|^2 + x^2|\mathbf{v}_s|^2 + 2x(1-x)|\mathbf{v}_0||\mathbf{v}_s|\cos\vartheta} \,, \tag{14}$$

where $\mathbf{v}_0 = \mathbf{v}_\odot \cos l$ and $\mathbf{v}_s$ are the solar and the source velocities transverse to the line of sight and $\vartheta$ the angle between them, whereas $l$ denotes the Galactic longitude. The solar velocity transverse to the Sun-Galactic centre line is denoted by $\mathbf{v}_\odot$, with $|\mathbf{v}_\odot| \simeq 220$ km s$^{-1}$. The distribution of the transverse velocity of the lens thus is

$$g_T(v_T, \vartheta)\, dv_T d\vartheta = \frac{1}{\pi v_D^2}\, v_T\, \exp\left(\frac{-(\mathbf{v_T} - \mathbf{v_t})^2}{v_D^2}\right) dv_T d\vartheta \,, \tag{15}$$

with a velocity dispersion $v_D \simeq 30$ km s$^{-1}$ in the disk (Paczyński 1991).

Due to the relative position $\gamma$ Nor and $\vartheta$ Mus are approximately moving towards us, whereas $\gamma$ and $\beta$ Sct are moving away from us. Hence, we will neglect the dispersion in the transverse velocity for sources located in these particular fields towards the spiral arms. We take into accout the dispersion velocity of the lenses in the disk using an expression as given in Eq.(13) but with a velocity dispersion $v_D \simeq 30$ km s$^{-1}$.

## 3. Mass and time moments

### *3.1. Optical depth and differential number of events*

To estimate the microlensing probability one introduces the optical depth $\tau_{opt}$ defined as

$$\tau_{opt} = \int_0^1 \frac{4\pi G}{c^2} \rho(x) D^2 x(1-x)\, dx \,, \tag{16}$$

with $\rho(x)$ the mass density at the distance $s = xD$ from the observer along the line of sight. $\tau_{opt}$ is the probability that a source is found within the Einstein radius $R_E$ of a lens, where $R_E$ is given by

$$R_E^2 = \frac{4GMD}{c^2} x(1-x) \equiv r_E^2 \mu x(1-x) \,, \tag{17}$$

with $x = s/D$; $D$ and $s$ are the distances to the source and the lens, respectively.

The optical depth is independent of the mass function of the lensing objects. To get the number of microlensing events one introduces the differential number of microlensing events (De Rújula et al. 1991, Griest 1991) :

$$dN_{ev} = N_* t_{obs} u_{\mathrm{TH}} 2 v_T f_T(v_T) D r_E \sqrt{\mu x(1-x)}\, \frac{dn}{d\mu} d\mu dv_T dx \,, \tag{18}$$

assuming an experiment that monitors $N_*$ stars during a period $t_{obs}$. This quantity yields the number of microlensing events with a magnification above a certain threshold $A_{\mathrm{TH}}$ (where $A_{\mathrm{TH}} = (u_{\mathrm{TH}}^2 + 2)/(u_{\mathrm{TH}}(u_{\mathrm{TH}}^2 + 4))$, $A_{\mathrm{TH}} = 1.34$ for $u_{\mathrm{TH}} = 1$).

### 3.2. Method of mass moments

A systematic way to describe the relevant quantities in a microlensing experiment is the method of mass moments (De Rújula et al. 1991), which are defined as

$$< \mu^m >= \int_{\mu_{min}}^{\mu_{up}} d\mu\, \epsilon_n(\mu)\, \frac{dn_0}{d\mu}\, \mu^m\,, \tag{19}$$

with $m = (n+1)/2$ and

$$\epsilon_n(\mu) \equiv \frac{\int dN^*_{ev}(\bar{\mu})\, \epsilon(T)\, \tau^n}{\int dN^*_{ev}(\bar{\mu})\, \tau^n}\,. \tag{20}$$

The sampling efficiency $\epsilon(T)$ is given by the experiment and $\tau = (v_i/r_E)T$, where $T$ is the time scale of the observed event (for which we adopt the definition that it is the time needed to cross the Einstein radius) and $v_i$ stands for the dispersion velocity in the bulge, disk or halo. $\epsilon_n(\mu)$ is called efficiency function and measures the fraction of the total number of microlensing events that, for a fixed MACHO mass $M = \mu M_\odot$, meet the condition $T_{min} \leqslant T \leqslant T_{max}$. $dN^*_{ev}(\bar{\mu})$ is defined as $dN_{ev}$ with, however, $dn_0/d\mu$ assumed to be a delta function $\delta(\mu - \bar{\mu})$. In other words, $\epsilon_0(\mu)$ indicates how efficient the experiment is to detect a MACHO with a given mass $M = \mu M_\odot$.

$< \mu^m >$ is related to the cumulative $n^{th}$ moment of $\tau$ constructed from the observations as follows

$$< \tau^n >= \sum_{\text{events}} \tau^n\,. \tag{21}$$

Due to the insertion of $\epsilon_n(\mu)$, the theoretical expression for the time moment

$$< \tau^n >= \int dN_{ev} \epsilon_n(\mu) \tau^n \tag{22}$$

factorises as follows

$$< \tau^n >= V u_{TH} \gamma(m) < \mu^m > \;, \tag{23}$$

with

$$V \equiv 2 N_* t_{obs} D r_E v_i\,. \tag{24}$$

$\gamma(m)$ is a quantity defined by the model, which depends on the spatial and the velocity distributions.

The mass moment $< \mu^m >$ is related to $< \tau^n >$, as given from the measured values of $T$, by

$$< \mu^m >= \frac{< \tau^n >}{V u_{TH} \gamma(m)}\,. \tag{25}$$

Some moments are directly related to physical quantities: the number of events is $N^{\rm obs}_{ev} =< \tau^0 >$. The mean local density of MACHOs (number per pc$^3$) is $< \mu^0 >$ and the average local mass density in MACHOs (solar masses per pc$^3$) is $< \mu^1 >$. Thus the mean MACHO mass is given by

$$\frac{< \mu^1 >}{< \mu^0 >} = \frac{< \tau^1 >}{< \tau^{-1} >}\, \frac{\gamma(0)}{\gamma(1)}\,, \tag{26}$$

in units of solar masses, where $< \tau^1 >$ and $< \tau^{-1} >$ are determined through the observed microlensing events. The average event duration $< T >$ can be expressed as follows

$$< T >= \frac{r_E}{v_i}\, \frac{< \mu^1 >}{< \mu^{1/2} >}\, \frac{\gamma(1)}{\gamma(1/2)}\,, \tag{27}$$

where again $i$ stands for the different components of the Galactic model.

### 3.3. Sources in the Galactic centre

Due to the extension of the bulge one has to take into account that the number density of possible source stars varies with distance $D$. This effect has to be taken into account in the calculation of the optical depth and the number of microlensing events. Following Kiraga & Paczyński (1994), the volume of space varies with distance as $D^2 dD$ and the number of detectable stars as $D^{2\beta}$, assuming that the fraction of stars brighter then some luminosity $L$ is proportional to $L^\beta$, where $\beta$ is a constant. In the following we will use a power-law luminosity function $\sim L^{-1}$ (i.e. $\beta = -1$), which is appropriate for main sequence source stars. An observable quantity towards the bulge, which we shall generically denote as $g_B$, is then obtained as

$$g_B = \frac{\int_0^\infty \varphi(D) g(D) dD}{\int_0^\infty \varphi(D) dD}\,, \tag{28}$$

with $\varphi(D) = \rho_B D^{2+2\beta}$ and $g(D)$ an observable quantity as for instance $\tau(D)$ or $N_{ev}(D)$. $\rho_B$ is the number density of stars as given in Eq.(1) and also varies as a function of $D$.

Accordingly, Eq.(22) and the subsequent relations which define the moments get modified, due to the additional integration over the distance $D$. It is, therefore, necessary to use the time $T$ instead of $\tau$ (which via $r_E$ depends on $D$). Otherwise, however, the calculation goes through similarly and the factorization of the mass moments is again achieved. Indeed, the $D$ dependence in the efficiencies $\epsilon_n(\mu)$ is negligible as we checked numerically.

Eq.(22) then becomes

$$< T^n >= \tilde{V}(n) \tilde{\gamma}(m) < \mu^m > \tag{29}$$

with

$$\begin{aligned} \tilde{V}(n) \;&=\; 2 N_* t_{obs} u_{TH} \left[\frac{2}{c}\sqrt{G M_\odot}\right]^{n+1} v_i^{1-n} \\ &=\; 2\left(4.4\times 10^{-7}\right)^{n+1} \times 10^{6n-6} \times \\ &\quad N_* u_{TH} \left(\frac{t_{obs}}{1\ \text{year}}\right) \left(\frac{v_i}{\text{km s}^{-1}}\right)^{1-n} \end{aligned} \tag{30}$$

$$\text{and}\;\; \tilde{\gamma}(m) \;=\; \frac{1}{N_B} \int \rho_B D^{m+3+2\beta} \gamma(m) dD\,, \tag{31}$$

where $N_B = \int_0^\infty \varphi(D) dD = \int_0^\infty \rho_B D^{2+2\beta} dD$.

On the other hand $< T^n >$ is determined from the observations by $< T^n >= \sum T^n$ ($T$ given in days). Thus, the mean

mass towards the bulge turns out to be

$$\frac{<\mu^1>}{<\mu^0>} = \frac{(v_i c)^2}{4GM_\odot}\frac{<T^1>}{<T^{-1}>}\frac{\tilde{\gamma}(0)}{\tilde{\gamma}(1)} = 5.35\left(\frac{v_i}{\mathrm{km\,s^{-1}}}\right)^2\frac{<T^1>}{<T^{-1}>}\frac{\tilde{\gamma}(0)}{\tilde{\gamma}(1)} \quad (32)$$

and the event duration is

$$<T> = \frac{2\sqrt{GM_\odot}}{v_i c}\frac{\tilde{\gamma}(1)}{\tilde{\gamma}(1/2)}\frac{<\mu^1>}{<\mu^{1/2}>} = 158\left(\frac{v_i}{\mathrm{km\,s^{-1}}}\right)^{-1}\frac{\tilde{\gamma}(1)}{\tilde{\gamma}(1/2)}\frac{<\mu^1>}{<\mu^{1/2}>}\ \mathrm{days}\,. \quad (33)$$

We now turn to the computation of the $\gamma(m)$, which enter into Eq.(31). For microlensing events towards the bulge, we have to distinguish between two cases: a) both the source and the lens are located in the bulge (bulge-bulge event), b) the source belongs to the bulge and the lens to the disk (bulge-disk event). We suppose the velocity distribution of sources and lenses in the bulge to be Maxwellian as given by Eq.(13). In this case the relative motion between observer and source can be neglected and the $\gamma(m)$-function as defined in Eq.(23) through the mass moments is given by

$$\gamma_{BB}(m) = \Xi(2-m)\hat{H}(m)\,, \quad (34)$$

where

$$\hat{H}(m) = \int_0^1 (x(1-x))^m\,\frac{\rho_B(x)}{\rho_{\circ B}}dx \quad (35)$$

$$\Xi(2-m) \equiv \int_0^\infty d\nu\int_0^{2\pi} d\vartheta\left(\frac{v_T(\nu)}{v_B}\right)^{1-n} f_{T,B}(\nu,\vartheta) \quad (36)$$

For lenses belonging to the disk, the transverse velocity distribution is given by Eq.(15), and we get

$$\gamma_{BD}(m) = 2\int_0^{2\pi} d\vartheta\int_0^\infty dv_s f_{T,B}(v_s,\vartheta) \times \int_0^1 dx\,\frac{\rho_D(x)}{\rho_{\circ D}}\,[x(1-x)]^m\,\mathrm{e}^{-\eta^2} \times \int_0^\infty dy\,y^{3-2m}I_0(2\eta y)\,e^{-y^2}\,. \quad (37)$$

with $y = v_T/v_D$, and $\eta = v_t/v_D$. The index $D$ labels the disk, $v_D \approx 30\ \mathrm{km\,s^{-1}}$ is the dispersion velocity in the disk and $I_0$ is the modified Bessel function of order 0 defined as

$$I_0(x) = \frac{1}{\pi}\int_0^\pi e^{x\,\cos(\beta)}\,d\beta\,. \quad (38)$$

The source stars belong to the bulge and are supposed to follow the distribution $f_{T,B}(v_s,\vartheta)$ as given in Eq.(11).

### *3.4. Sources in the spiral arms and in the halo*

If the source as well as the lens is located in the disk, the small relative transverse velocity between them can be neglected, as explained above and we can assume a Maxwellian velocity distribution as given in Eq. (13). We can perform the $\vartheta$ integration and the corresponding $\gamma(m)$-function turns out to be as in Eq.(34), with Eq.(36) replaced by

$$\Xi(2-m) \equiv \int_0^\infty\left(\frac{v_T}{v_D}\right)^{1-n} f_{T,H}(v_T)dv_T = \Gamma(2-m)\,, \quad (39)$$

where $v_D \simeq 30\ \mathrm{km\,s^{-1}}$ is the dispersion velocity in the disk. Sources in the halo, like LMC, SMC or dwarf galaxies are more distant, and thus the relative motion between observer and source can also be neglected in leading order. Assuming in addition a Maxwellian velocity distribution the resulting $\gamma(m)$-function turns out to be as in Eqs. (34) and (39), with $v_D$ replaced by $v_H$, the dispersion velocity in the halo.

## 4. Lensing towards the Galactic bulge and some spiral arm regions

Let us apply the formalism presented above to different lines of sight towards the bulge and some fields in the spiral arms. In the bulge we focus on the direction of Baade's Window ($l = 1^\circ$, $b = -3.9^\circ$) and in the spiral arms towards $\gamma$ Nor ($l = -28.8^\circ$, $b = -2.7^\circ$), where some microlensing events have already been observed.

### *4.1. Optical depth*

In Fig. 1 the optical depth $\tau$ is shown as a function of the Galactic longitude $l$ for a fixed value of the latitude $b = -3^\circ$. The approximate position of $\gamma$ Nor, $\gamma$ and $\beta$ Sct and Baade's Window are indicated. The idea is just to give an impression of the global behaviour of the optical depth towards Baade's Window and the spiral arms. The values towards these targets are given below.

The dashed line $\tau_{BB}$ is the contribution due to lenses and sources located in the bulge for which we have taken into account the varying distances. One clearly sees that it is the major contribution to the optical depth in the range $-8^\circ \lesssim l \lesssim 10^\circ$. The tilt angle $\Phi_\circ$ (for which we assume $\Phi_\circ = 20^\circ$) of the bar major axis with respect to the Sun-Galactic centre line leads towards the bulge to a slight asymmetry in the optical depth with respect to $l = 0^\circ$.

The curve labeled by $\tau_B$ is the total optical depth, which contains also the contribution due to lenses located in the disk and the source star in the bulge for which we again take into account the varying distances.

Towards Baade's Window ($l = 1^\circ$, $b = -3.9^\circ$) the total optical depth $\tau_B = 1.9 \times 10^{-6}$ is the sum of the disk $\tau_D = 0.7 \times 10^{-6}$ and the bulge $\tau_{BB} = 1.2 \times 10^{-6}$ contributions. The bulge contribution is about 1.7 times more important than the disk. This value is in reasonable agreement with the optical depth found by the MACHO group: $\tau_B = (2.4 \pm 0.5) \times 10^{-6}$ (Alcock et al. 1997a). The OGLE collaboration found a somewhat higher value: $\tau_B = (3.3 \pm 1.2) \times 10^{-6}$ (Udalsky et al.

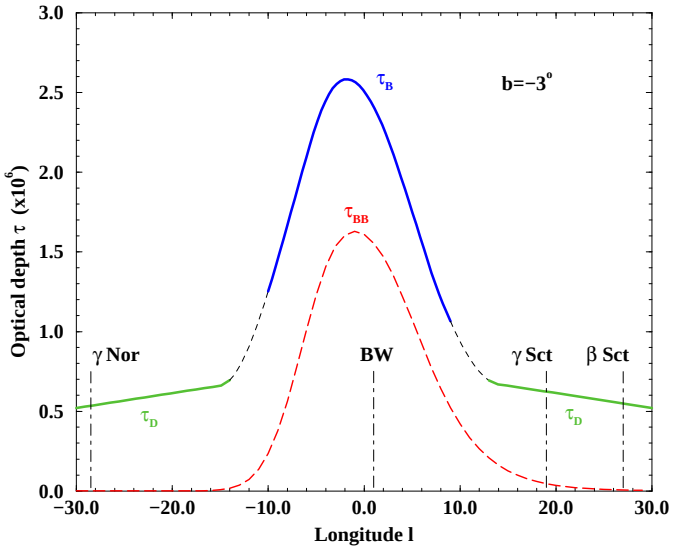


**Fig. 1.** The optical depth $\tau$ (in units of $10^{-6}$) for the different components of the Galaxy as a function of the Galactic longitude $l$ for a fixed latitude $b = -3^{\circ}$. For the disk contribution ($\tau_D$) the distance is fixed at 8 kpc, while for the bulge contribution ($\tau_B$) we integrated over the distance distribution of the lenses and sources. $\tau_{BB}$ denotes the fraction of $\tau$ for source and lens located in the bulge (where the tilt angle $\Phi_0$ is taken to be $20^{\circ}$). The dotted lines are just an interpolation between the bulge and the disk regions. The approximate positions of $\gamma$ Nor, $\gamma$ and $\beta$ Sct and Baade's Window (BW) are indicated.

1994). We notice that it has been pointed out that the contribution of unresolved stars might be quite significant and as a result imply that the measured optical depth is overestimated (Alard 1997). If this is the case the measured value has to be regarded as an upper limit to the true value.

By varying the tilt angle from $15^{\circ}$ to $30^{\circ}$ the optical depth $\tau_{BB}$ for the bulge decreases from $1.33 \times 10^{-6}$ to $0.97 \times 10^{-6}$ (and the total optical depth from $2.02 \times 10^{-6}$ to $1.68 \times 10^{-6}$).

Outside the bulge region both the source and the lens belong to the disk population and the total optical depth is labelled in Fig. 1 by $\tau_D$. In this case we assume all source stars to be located at the same distance of 8 kpc.

Observations towards 27 different fields in the spiral arms are included in the scientific program of the EROS II (Derue et al. 1999) and the MACHO teams. The 27 fields observed by EROS II belong to 4 dense regions of the spiral arms: $\gamma$ Sct, $\beta$ Sct, $\gamma$ Nor and $\vartheta$ Mus. The star density lies between 400 000 and 700 000 stars per field, leading to about 10 millions observable stars (Mansoux 1997). Their average Galactic coordinates, distances, observed number of stars, number of events found so far during an observation time of 1.7 years and the calculated optical depth are reported in Table 1.

EROS II found altogether 3 events (see Table 1) and estimated an optical depth, averaged over the four directions, of $\tau = 0.38^{+0.53}_{-0.15} \times 10^{-6}$ (Derue et al. 1999). For comparison we get an averaged optical depth of $\tau = 0.42 \times 10^{-6}$ using our model, which is in good agreement with the EROS II value.

### *4.2. The mass functions*

Towards the bulge we compute the mass functions using the first year data of the MACHO collaboration taken in 1994. Observing during 190 days star fields with a total of 12.6 million source stars towards Baade's Window, they found 40 microlensing events (neglecting the double lens event).

Due to the limited amount of data, we make the Ansatz $dn_0/d\mu \sim C_i^1(\alpha_i)\mu^{-\alpha_i}$ and use then the mass moments to determine the parameters $\alpha$ and $\mu_{min}$. $C_i^1(\alpha_i)$ is defined by Eq.(9) and we assume a maximal mass ($\mu_{max}$) for the stars of $\sim 10 M_{\odot}$. The upper limit $\mu_{up}$ of the integration in Eq.(19) is set equal to 1 $M_{\odot}$, since more massive and thus brighter stars will not contribute much to microlensing events. To evaluate Eq.(19) we first have to calculate the efficiency functions defined by Eq.(20) using the sampling efficiency $\epsilon(T)$ as given by the MACHO team for their first year events towards the Galactic bulge.

We notice that one should also take into account the contribution due to unresolved stars, which for the bulge might be relevant and induces changes in the optical depth and the microlensing rate (Alard 1997; Han 1997). Indeed, if a faint unresolved star is lensed close enough to a resolved star, the event will be seen by the microlensing experiment and attributed to the brighter star. The blending biases the event towards a shorter duration, leading to an overestimate of the amount of these events. As a result the mass function will be shifted towards lower values of $\mu_{min}$. A quantitative estimate of the induced error on our results is, however, difficult, since it would require a detailed knowledge of the data analysis and the determination of the sampling efficiency. Hopefully, this information will be available when the new microlensing observations towards the bulge will be made available by the observational teams.

The mass moments as computed by Eq.(19) are compared to the corresponding time moments derived from the observed microlensing events through the expression given in Eq.(25). Thus with the mass moments, $< \mu^0 >$ and $< \mu^{1/2} >$, we get two equations, which then are solved with respect to the unknown quantities $\alpha$ and $\mu_{min}$. Further moments can be used for instance to check whether the values we obtain for $\alpha$ and $\mu_{min}$ are consistent. Since we do not know the fraction of the observed events due to lenses located in the bulge, respectively in the disk, we assume that this fraction is equal to the corresponding ratio of the optical depths hence $\tau_{BB}/\tau_B \simeq N_B/N_{tot} (\simeq 25.1/40)$. This assumption is well fulfilled if the mean event duration of the bulge and disk events are the same. We will then a posteriori verify if this condition is matched by the results we get and thus see whether our assumption is consistent.

With the above procedure we get for the parameters of the power-law mass function of the lenses in the bulge the values $\alpha = 2.0$ and $\mu_{min} = 0.012$ with $C_B^1 = 0.34\ M_{\odot}\ \mathrm{pc}^{-3}$. Similarly we can use the disk events to determine the mass function of the disk population to find again $\alpha = 2.0$ and instead a minimal mass of 0.021 $M_{\odot}$ with $C_D^1 = 9.86 \times 10^{-3}\ M_{\odot}\ \mathrm{pc}^{-3}$. The average durations we find are $\langle T_B \rangle = 20.5$ days and

$\langle T_D \rangle = 19$ days, respectively. Therefore we see that the assumption $\langle T_B \rangle \simeq \langle T_D \rangle$ is quite well verified.

Varying the tilt angle $\Phi_\circ$ between $15^\circ$ and $30^\circ$ the slope $\alpha$ for the bulge mass function slightly changes from 1.9 to 2.15 and the minimal mass $\mu_{min}$ from 0.009 to 0.023 whereas the number of bulge events decreases from 25 down to 22.7. The mean event duration for the bulge $\langle T_B \rangle$ changes accordingly from 22.1 to 19.1 days. Similar small changes occur in the corresponding numbers of the disk events. We thus see that our results are robust for reasonable values of the tilt angle.

Due to the above considerations on the unresolved stars, the values for $\mu_{min}$ we find have to be considered as a lower limit on the true values. We notice that a change in $\mu_{min}$ affects also the value of $\alpha$. Similar studies have also been performed with different methods by Han & Gould (1995) and Peale (1998,1999). They find somewhat different mass functions for the bulge, but again given the small amount of data at disposal the errors are still large and so no definite conclusions can be drawn. Recently, Reid et al. (1999) using observations from the Deep Near-Infrared Survey (DENIS) and the 2 Micron All-Sky Survey (2MASS) have suggested the presence of a local unknown population of free brown dwarfs with a mass function with minimal value as low as 0.01 $M_\odot$. If confirmed it may well be plausible to find this population also in the bulge.

### *4.3. Mass and time moments towards the bulge*

For the calculation of the mass and time moments towards the bulge we have to distinguish between the two cases, whether the lens is located in the bulge or in the disk, and to choose accordingly the appropriate velocity distribution as given by Eq.(11) or Eq.(15). The number of events and the event duration are defined by $N_{ev}^{obs} =< T^0 >$ and Eq.(34), respectively, where the moments of $T$ are given by Eq.(29).

Figure 2 shows the number of expected microlensing events as a function of the longitude for a delta mass distribution with $\mu_0 = 1$, assuming to monitor $10^6$ stars during an observation time of 1 year. The efficiency is taken to be 1. Again, as in the plot of the optical depth, it shows the global behaviour of the expected number of events towards the bulge and the spiral arm regions. The distance towards the spiral arms is kept fixed at 8 kpc and the latitude at $b = -3^\circ$.

$N_{ev,B}$ is the total number including also the contribution due to lenses located in the disk and sources in the bulge. For the latter we take into account the dependence on the distance as illustrated in Eq.(27). For the number of events towards the spiral arms, $N_{ev,D}$, the source is located in the spiral arms and the lenses belong to the disk population.

In Fig. 4 we plot the efficiency functions which are derived from the sampling efficiency $\epsilon(T)$ as given by the MACHO team towards Baade's Window. We recall that for instance $N_{ev}$ scales like $\sim v\ \mu^{-1/2}$, whereas $< T >$ as $v^{-1}\ \mu^{1/2}$. $N_{ev,BB}$ is the contribution due to the bulge (i.e. events with source and lens in the bulge).

Figure 3 shows the expected number of microlensing events assuming the power-law mass functions we found with the parameters as mentioned in Sect. 4.2. For this plot the same efficiency $\epsilon(T)$ as given by the MACHO team towards Baade's Window is assumed for all directions. All the other parameters are the same as the ones used in Fig. 2.

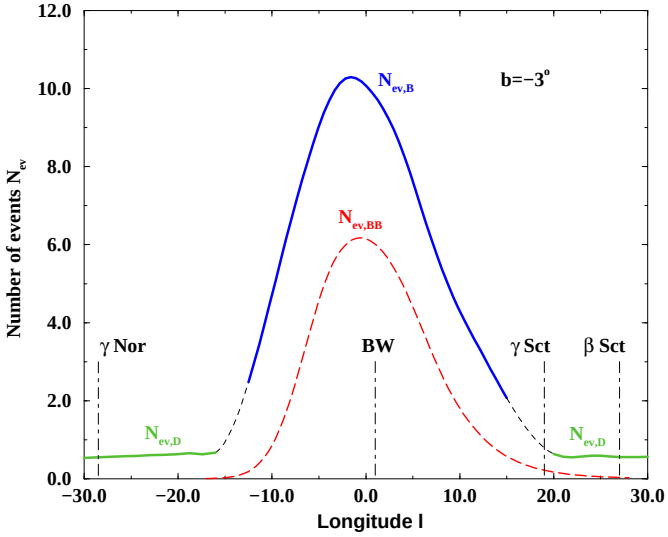


**Fig. 2.** The number of events for a delta mass distribution with $\mu_0 = 1$ as a function of the longitude with fixed latitude $b = -3^\circ$. The total exposure is assumed to be $10^6$ star-years. The $N_{ev,BB}$ curve (source and lens in the bulge) reflects the position of the bulge (tilted by $\Phi_0 = 20^\circ$), which is important in the range $-8^\circ \lesssim l \lesssim 10^\circ$. In this range, the total number (denoted by $N_{ev,B}$) is dominated by the events with the lens located in the bulge. Outside of this range the events $N_{ev,D}$ are due to sources located in the spiral arms and lenses in the disk population. The efficiency function $\epsilon_0(\mu)$ is assumed to be 1 in this plot.

Using the values for the various parameters as given in Sect. 2 and power-law mass functions with $\alpha = 2.0$, $\mu_{min,B} = 0.012$ for the bulge and $\mu_{min,D} = 0.021$ for the disk population, respectively, the number of events towards Baade's Window are consistently reproduced to be $N_{ev}$= 40.5. This is just the sum of $N_{ev,BB} = 25.0$ and $N_{ev,D} = 15.5$, which we get when considering 12.6 million source stars observed during 190 days as in the MACHO first year data. The mean event duration, as given by Eq.(34), is $< T >_B$= 20.5 days for bulge events and $< T >_D$= 19.0 days for disk events. These durations have to be compared with the actual observations of the reported 40 events with $< T_{obs} >$= 19.9 days. We thus see that the values for the durations we get using our model are in good agreement with the observed one. For the mean mass we get 0.091 $M_\odot$ for the lenses in the bulge and 0.124 $M_\odot$ for the lenses in the disk, respectively. Due to the sampling efficiency this value is actually an upper limit of the true value (when not taking into account the problem of the unresolved sources). Just for comparison the theoretical value we would get for the average mass in the bulge assuming the power-law mass function as mentioned in Sect. 4.2, with $\epsilon = 1$, is 0.054 $M_\odot$. As expected, this value is somewhat lower than the one inferred from the data.

| | $< l >$ | $< b >$ | $D$ kpc | $N_*$ ($\times 10^6$) | $N_{oe}$ | T (days) | $\tau_{tot}$ ($\times 10^6$) | $N_{ev}$ | $< T >$ (days) | $\gamma(0)$ | $\gamma(1/2)$ | $\gamma(1)$ |
|---|---|---|---|---|---|---|---|---|---|---|---|---|
| $\gamma$ Sct | 18.6 | -2.6 | 6.5 | 1.70 | 1 | 73 | 0.41 | 0.60 | 76.9 | 1.62 | 0.563 | 0.269 |
| $\beta$ Sct | 27 | -2.5 | 6.5 | 1.96 | 0 | - | 0.38 | 0.63 | 77.4 | 1.47 | 0.516 | 0.248 |
| $\gamma$ Nor | -28.8 | -2.7 | 8.0 | 3.01 | 2 | 98&70 | 0.56 | 1.29 | 86.5 | 1.42 | 0.504 | 0.244 |
| $\vartheta$ Mus | -53.6 | -1.8 | 7.0? | 1.77 | 0 | - | 0.32 | 0.47 | 80.9 | 1.07 | 0.379 | 0.184 |

**Table 1.** The distance $D$, the number of observed stars $N_*$ and the number of observed events $N_{oe}$ with their duration $T$ are given for $\gamma$ Sct, $\beta$ Sct, $\gamma$ Nor and $\vartheta$ Mus (Derue et al. 1999). The optical depth $\tau_{tot}$, the number of events $N_{ev}$ and the mean event duration $< T >$ are computed adopting the model outlined in Sect. 2 and a power-law mass distribution with $\alpha = 2.0$ and $\mu_{min} = 0.021$. The disk dispersion velocity is $v_D = 30$ km s$^{-1}$. We assume to observe $N_*$ stars during an observation time of 1.7 years with a sampling efficiency as given by the EROS II team.

| | $\tau_{tot}$ ($\times 10^6$) | $N_{ev}$ | $< T >$ (days) | $\bar{\mu}$ | $\tilde{\gamma}(0)$ | $\tilde{\gamma}(1/2)$ | $\tilde{\gamma}(1)$ |
|---|---|---|---|---|---|---|---|
| Bulge | 1.20 | 25.0 | 20.5 | 0.091 | $3.82 \times 10^2$ | $1.59 \times 10^4$ | $9.58 \times 10^5$ |
| Disk | 0.70 | 15.5 | 19.0 | 0.124 | $2.83 \times 10^5$ | $2.02 \times 10^6$ | $1.94 \times 10^7$ |
| Total | 1.90 | 40.5 | 19.9 | - | - | - | - |

**Table 2.** The optical depth, the number of events and the mean event duration towards Baade's Window are computed following the model outlined in the text. For the computation of $N_{ev}$ and $< T >$ we inserted the computed power-law mass functions with $\alpha = 2.0$ and $\mu_{min} = 0.012$ for the bulge and $\mu_{min} = 0.021$ for the disk. We assume an observation time of 0.52 years and $12.6 \times 10^6$ stars.

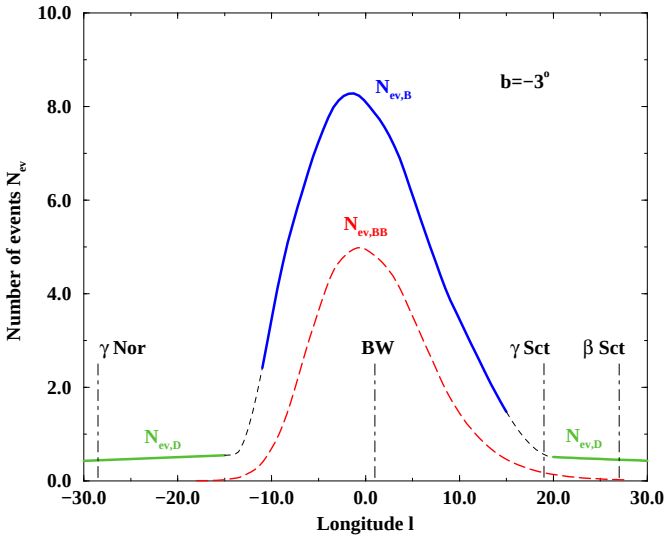


**Fig. 3.** The number of events for power-law mass functions with $\alpha = 2.0$ and $\mu_{min,B} = 0.012$ for the bulge and $\mu_{min,D} = 0.021$ for the disk population, respectively. The efficiency function of the MACHO collaboration is taken into account in the calculation to be able to directly compare with the experiment. The total exposure is taken to be $10^6$ star-years.

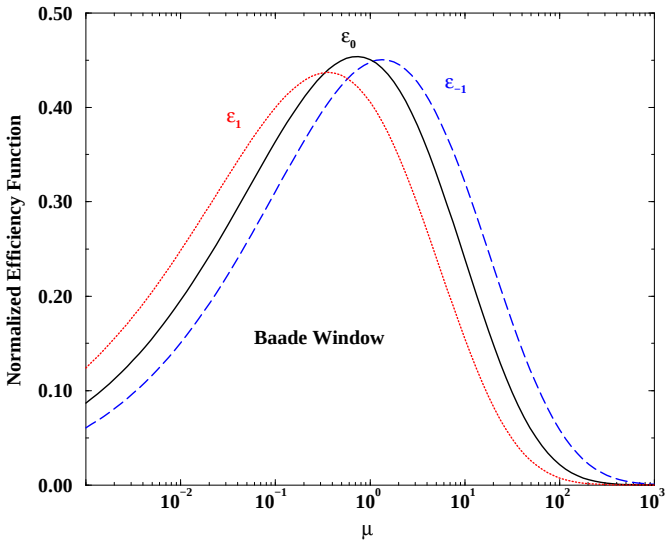


**Fig. 4.** Efficiency functions $\epsilon_n(\mu)$ $(n = -1, 0, 1)$ derived from the sampling efficiency towards Baade's Window of the MACHO collaboration.

### *4.4. Mass and time moments towards the spiral arms*

The corresponding results for the various directions in the spiral arms are summarized in Table 1. To calculate the number of expected events we assume the power-law mass function obtained for the disk and the number of observed stars (indicated in Table 1) and the observation time of 1.7 years as given by the EROS II experiment. Moreover, we adopted the sampling efficiencies quoted by EROS II (Derue et al. 1999).

For the $\gamma$ Nor direction we studied how the results change by varying the various parameters, which enter the calculation of the number of events and their duration. As a first point we notice that changing the maximal mass $\mu_{max}$ of the source stars or the maximal mass $\mu_{up}$ of the lenses in the power-law model has a very minor influence on the subsequent results and can, therefore, be neglected. By varying the minimal mass $\mu_{min}$ be-

tween 0.005 and 0.05 keeping all other parameters fixed, $N_{ev}$ decreases from 1.7 to 1.0 and the mean event duration $< T >$ increases from 63 to 106 days. If the slope value $\alpha$ of the power-law varies between 1.7 and 2.5 (for $\mu_{min} = 0.021$), the number of events increases from 0.95 to 1.9 events with a corresponding duration decrease from 101 to 69 days.

If we assume instead of a power-law a delta mass distribution with most probable masses $\mu_{0D} = 0.124$ (or $\mu_{0B} = 0.091$) we get 3.1 (3.5) events with a duration of 87 (76) days.

Another important parameter is the dispersion velocity in the disk. Changing its value between 20 and 40 km s$^{-1}$, $N_{ev}$ increases from 0.86 to 1.7 and $< T >$ decreases from 130 to 65 days, respectively.

We thus see that the small number of observed events does not yet constrain very much the different parameters entering the model. Nevertheless, once more data will be available the allowed range for the parameters will be narrowed considerably and in this respect the method of mass moments will be very useful leading to a much better knowledge of the structure of the bulge and the disk of our Galaxy.

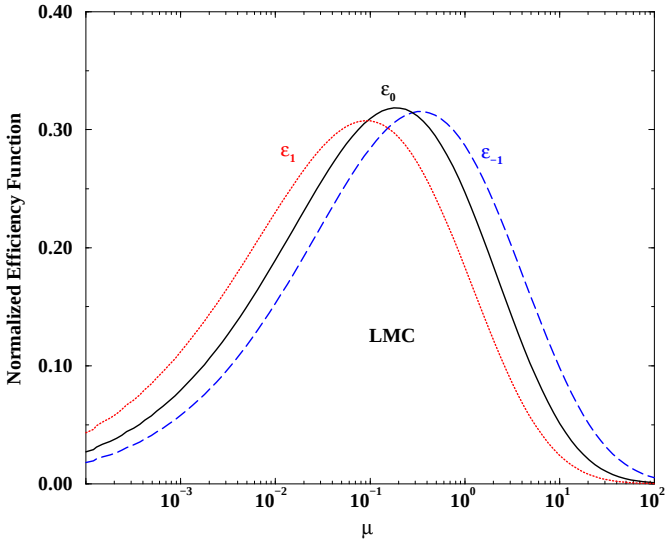


**Fig. 5.** Efficiency functions $\epsilon_n(\mu)$ $(n = -1, 0, 1)$ derived from the sampling efficiency towards the LMC of the MACHO collaboration.

## 5. Lensing towards halo targets

Two important unknowns in Galactic models are the shape of the halo and the velocity distribution of the halo objects. Although it is widely believed that dark matter halos are not spherical, a systematic explanation how to generate deviations from spherical symmetry is not yet available. To investigate how the presence of massive Galactic companions such as the Magellanic Clouds may induce a flattening of the halo, and to test how such a presence could influence the isotropy of the dispersion velocity (Holder & Widrow, 1996) we performed a N-body simulation which yields, as a result, the density and velocity distribution of the halo objects. For the details we refer to the Appendix. Of course our results have to be taken as an illustration, given also the crude approximations we use. For the targets towards different halo directions we will adopt the flattening parameter $q_H$ and the dispersion velocities as obtained from the numerical simulation. These values are tabulated in Table 3.

### *5.1. Magellanic Clouds*

The optical depth towards the LMC for the spherical halo model is $\tau_{\rm LMC} \simeq 5.33 \times 10^{-7}$ ($4.93 \times 10^{-7}$ due to the halo and $0.40 \times 10^{-7}$ due to the disk contribution), where we used the standard parameters for the LMC ($l = 280.5°$, $b = -32.9°$, $D = 50\,$kpc). For the halo core-radius we adopt $R_C = 5.6\,$kpc. The measured value, as reported by the MACHO collaboration, is: $\tau_{\rm MACHO} \simeq 2.4^{+1.4}_{-0.9} \times 10^{-7}$, which corresponds to about 50% of the above predicted value for a standard spherical halo (Alcock et al. 1997a). Similarly, towards the SMC ($l$=302.8, $b$=-44.3, $D$=63 kpc) the calculated optical depth is $\tau_{SMC} \simeq 7.39 \times 10^{-7}$ ($7.08 \times 10^{-7}$ and $0.31 \times 10^{-7}$ for the halo and disk contribution, respectively).

The MACHO team found two microlensing events towards the SMC, one being a binary event (Alcock et al. 1997c, Palanque-Delabrouille et al. 1997, Udalski et al. 1997). Using a simple estimate for the total exposure and assuming for $\epsilon$ the corresponding LMC efficiency, they estimate the optical depth towards the SMC to be roughly equal to the optical depth towards the LMC. A similar conclusion has been also reached by the EROS II team, which quotes a value $\tau \simeq 3.3 \times 10^{-7}$ (Perdereau 1998). To get a ratio $\tau_{LMC}/\tau_{SMC}$ of about 1, a halo flattening of almost $q_H = 0.5$ is required. However, it might well be that the events found so far are due to lenses in the SMC itself (in particular this is the case for the binary event), in which case the above conclusions on $\tau$ are no longer valid.

From the 6 events (excluding the binary lens event and an event which is considered being only marginally consistent with microlensing) published by the MACHO team for their first two years observations, we find with the method of mass moments for a spherical halo model an average mass of 0.26 $M_\odot$ (Jetzer 1996). If we assume for the dispersion velocity 191 km s$^{-1}$ as found in the N-body simulation instead of 210 km s$^{-1}$ as used for the spherical halo, we get for the average mass a slightly lower value of 0.22 $M_\odot$.

Adopting the values for the first two years observation of the MACHO team towards the LMC, namely a total exposure of 2.1 years for $8.5 \times 10^6$ stars with the detection threshold $u_{TH} = 0.661$ and the calculated efficiency functions $\epsilon_n(\mu)$ from the MACHO sampling efficiency, we compute the expected number of events and the mean event duration for a $q_H = 0.8$ flattened halo. A delta mass function with $\mu_H = 0.22$ is used for the halo and the computed power-law mass function ($\mu_{min} = 0.021$, $\alpha = 2.0$) for the disk. We find $N_{ev} = 12.2$ (where the halo contributes with $N_H = 10.4$ and the disk with $N_D = 1.8$) and $< T >_{LMC} = 32.5$ days ($< T >_H = 34.1$ days and $< T >_D = 23.1$ days, respectively). Using a spher-

ical halo with $v_H = 210$ km s$^{-1}$ we find $N_{ev} = 14.5$ and $< T >_{LMC} = 30.3$ days. We see that the flattening of the halo and the change in the velocity dispersion reduces, although slightly, the number of expected events, while the average duration increases.

The value for $N_{ev}$ is valid assuming a halo made entirely of MACHOs. For a 50% contribution of MACHOs as implied from the optical depth we thus expect about 6 events, which compares well with the 6 observed events. The event duration has to be compared with the measured 35.5 days of the 6 observed events. It is noticeable that we expect about two events as due to the disk contribution. In addition LMC self-lensing may also contribute with some events (Salati et al. 1999), which we do not take into account in our calculation. Indeed, the fraction of the optical depth due to self-lensing is still controversial, although a recent analysis of Gyuk et al. (1999) comes to the conclusion that it contributes at most 10-20% to the observed optical depth. Thus the bulk of the events should still come from MACHOs located in the halo. Given this mixing of different populations in the events one has to be careful with the interpretation of the average mass, since it is derived under the assumption that all events are due to MACHOs in the halo, which is probably not the case.

### *5.2. Dwarf galaxies*

The LMC and the SMC are the only two targets in the halo with a sufficiently high number of stars which can be resolved such that the method of microlensing can be applied. Other targets such as the satellite dwarf galaxies, can still be used for microlensing observations however, due to their size and distance much less stars can be resolved. One could envisage in this case to use the pixellensing method instead. With this method one can look at rich fields of stars which are located further out and thus are not resolvable. The method, proposed by Crotts (1992) and Baillon et al. (1993), has proven to work with M31 and so it is conceavable to extend the observations to some of the several satellite dwarf galaxies of the Milky Way. Such observations would be very useful, since they would allow to test other directions as the ones towards the LMC and the SMC.

In Table 3 we report the relevant quantities for some possible targets in the halo and the neighbourhood of the Milky Way, for which we assumed an extension of the halo of 150 kpc (Bahcall 1996) and a flattening parameter of $q_H = 0.8$. For the number of events and the mean event duration a delta distribution with the mass value $\mu_0 = 1$ is assumed. The dispersion velocity is taken from the simulation presented in the Appendix. The total exposure is taken to be $10^6$ star-years and the efficiency is set equal to 1. The number of events is determined under the assumption of a halo made entirely of MACHOs.

In comparison for a standard spherical halo with $v_H = 210$ km s$^{-1}$ we would expect about 20% more events, but with a duration of about 7% shorter. Similar results have also been found by De Paolis et al. (1996) in the framework of halo models with anisotropy in the velocity space.

Other possible targets from which interesting Galactic structure can be extracted are globular clusters, for which we refer to the papers by Gyuk & Holder (1998), Rhoads & Malhotra (1998) and Jetzer et al. (1998).

## 6. Discussion

We studied in detail microlensing towards different lines of sight which are promising to obtain information about the structure of our Galaxy using the method of mass moments. With the first year MACHO data in the direction of the Galactic centre we determined the mass functions of lenses in the bulge and the disk assuming a power-law. The obtained mass functions are both slightly less steep continuations of the Salpeter IMF down to the brown dwarf region, with a minimal mass of $\simeq 0.012\ M_\odot$ for the bulge and $\simeq 0.021\ M_\odot$ for the disk with a slope $\alpha \simeq 2.0$ for both cases. By varying the tilt angle of the bulge in the range from $15^\circ$ to $30^\circ$, which is suggested by the most recent models, the inferred mass functions do practically not change.

As next we computed the expected number of events and their duration for different targets in the spiral arms, which have been explored by the EROS II collaboration. Assuming the same mass function as derived for the disk we get event durations which are in good agreement with the values found for the 3 events observed towards $\gamma$ Nor and $\gamma$ Sct. On the other hand, the calculated number of events turns out to be somewhat smaller, although given the few events found so far the uncertainties are still large and, moreover, the theoretical values vary in a significant way even for slight changes of the parameters such as the velocity dispersion.

Microlensing towards fields in the spiral arms is an important tool to explore the structure of the disk and especially its mass function and dispersion velocity. The method of mass moments can be used to get in a systematic way important information from the data, as soon as a sufficient number of events will be observed, which is certainly the case towards Baade's Window. It is also important to further develop the Galactic models, especially the modelling of the spiral arms and the motion of the stars inside them. Comparison then with the data will lead to stringent constraints on the model.

To obtain a qualitative understanding how the presence of massive companions may influence the Galactic halo, we performed a N-body simulation of the halo from which we obtained a halo flattening parameter $q_H \simeq 0.8$ as well as an idea how the dispersion velocity can vary as a function of the observational direction. The parameters from the simulation were then used to compute the optical depth, the expected number of events and the duration for several targets in the halo of our Galaxy.

Although most of the results we obtained have to be considered as preliminary and will soon improve due to many new events which will be available, we find that within the adopted model for the Galaxy the agreement between the computed values for the optical depth, the expected number of microlensing

| target | distance (kpc) | l | b | $\tau_{tot}$ ($\times 10^7$) | disp. vel (km s$^{-1}$) | $N_{ev}$ | $< T >$ (days) | $\gamma(0)$ ($\times 10^2$) | $\gamma(1/2)$ ($\times 10^2$) | $\gamma(1)$ ($\times 10^2$) |
|---|---|---|---|---|---|---|---|---|---|---|
| LMC | 50 | 280.5 | -32.9 | 4.8 | 191 | 1.5 | 73 | 28.48 | 8.60 | 3.71 |
| SMC | 63 | 302.8 | -44.3 | 6.1 | 195 | 1.8 | 78 | 25.69 | 7.34 | 3.04 |
| NGC 205 | 690 | 120.7 | -21.1 | 7.3 | 344 | 2.8 | 59 | 6.82 | 1.64 | 0.62 |
| NGC 147 | 690 | 119.8 | -14.3 | 7.8 | 195 | 1.9 | 96 | 8.02 | 1.81 | 0.65 |
| Fornax | 230 | 237.3 | -65.7 | 6.2 | 195 | 1.4 | 102 | 7.72 | 1.65 | 0.57 |
| Draco | 60 | 86.4 | 34.7 | 5.1 | 192 | 1.5 | 77 | 22.73 | 6.54 | 2.74 |
| Ursa Minor | 80 | 104.9 | 44.9 | 5.0 | 184 | 1.3 | 89 | 15.06 | 3.95 | 1.57 |
| Ursa Major | 120 | 202.3 | 71.8 | 5.3 | 175 | 1.2 | 106 | 9.21 | 2.10 | 0.76 |
| Leo I | 230 | 226.0 | 49.1 | 6.2 | 174 | 1.3 | 115 | 7.38 | 1.60 | 0.56 |
| Leo II | 230 | 220.1 | 67.2 | 6.0 | 176 | 1.2 | 113 | 7.48 | 1.59 | 0.55 |
| NGC 2419 | 60 | 180.4 | 25.3 | 3.4 | 202 | 1.1 | 70 | 15.53 | 4.33 | 1.80 |
| Sagittarius | 24 | 5 | -15 | 12.6 | 205 | 5.2 | 56 | 143.29 | 53.74 | 26.92 |

**Table 3.** Optical depth, number of events and event duration for different targets in the halo and the neighbourhood of the Milky Way. For the number of events and the mean event duration a delta distribution with the mass value $\mu_0 = 1$ is assumed. The total exposure is taken to be $10^6$ star-years. The halo is assumed to be flattened with $q_H = 0.8$ and the values for the dispersion velocity are taken from the N-body simulation.

events and the observation is quite good, given also the uncertainties in various important parameters.

*Acknowledegments.* L.G. and M.S. are partially supported by the Swiss National Science Foundation. We thank M. Moniez and R. De Ritis for useful discussions. Moreover we are grateful to the referee C. Alard for several useful comments, which helped to improve the paper.

## Appendix A: N-body Simulation of the Galactic Halo

In this Appendix we present a N-body simulation of the galactic halo. The simulation aims to give a qualitative understanding of how and to what extent the presence of massive bodies like the LMC and SMC influence the shape and the velocity dispersion in the halo. These latter quantities are relevant for microlensing. We stress that our simulation has to be considered as a first step and that the results we find should be regarded as illustrative.

### *A.1. The Model*

Our model consists of three massive point particles, which represent the Galaxy, the LMC and the SMC, respectively. The central mass is assumed to be $5 \times 10^{11}\, M_\odot$, while we set for the LMC-mass $6 \times 10^9\, M_\odot$ and for the SMC-mass $1.5 \times 10^9\, M_\odot$ (Westerlund 1990). In the field of these three gravitating bodies we let evolve a halo consisting of $2.8 \times 10^7$ test-particles for about $9.5 \times 10^9$ years. The time resolution of the simulation is $30\,000$ time steps of $10^{13}$ s ($3.17 \times 10^5$ years) each. The halo is discretised into $50^3$ equidistant bins with respect to spherical coordinates $(r, \vartheta, \varphi)$, hence, yielding an average population of $\sim 200$ MACHOs per bin. To keep the problem clean and simple, we do not yet include an extended (oblate or prolate) massive halo into the gravitational potential hence, we ignore any possible backreaction of the halo on the clouds. As a consequence of our test-particle approach all the results will be valid only up to a normalization constant depending on the total mass of the halo.

The initial conditions for the Magellanic Clouds are chosen such that at the end of the simulation the locations and the velocities are close to the observed values of the LMC and SMC (Lin, Jones & Klemola 1995). However, since the many-body problem depends crucially on the initial values and we made some compromises to avoid pathological orbits due to close encounters between the LMC and the SMC, the final location does not exactly match the real one.

The initial spatial distribution of the halo objects mimics an isothermal sphere with a cut-off radius of $100\,$kpc. The initial velocities were chosen to be Keplerian in magnitude and random in direction. We assume a total zero angular momentum halo in order to not overestimate the halo flattening due to the presence of the Magellanic Clouds.

To test the reliability of the results we performed some control runs, varying the initial conditions as well as the duration and the time resolution of the simulation. We found that the results are stable unless significant anisotropies are introduced in the initial data. A time duration slightly less than a Hubble time is sufficient for the developement of a steady configuration.

### *A.2. The Results*

The simulation yields the entire phase-space of all halo objects. Hence, we are able to extract all halo parameters entering in gravitational microlensing, which are independent of the sources in relative units with the exception of the lens mass function.

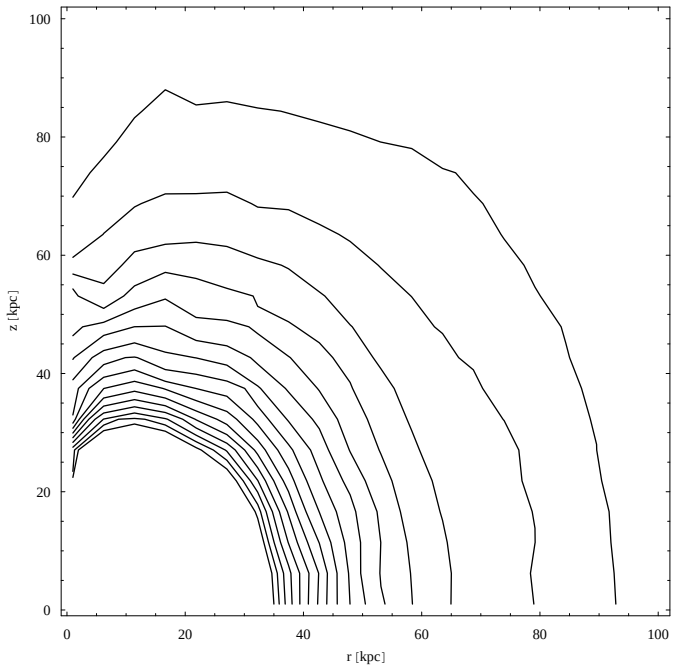


**Fig. A.1.** Isocontour lines of the MACHO-density in cylindrical coordinates. The final configuration is sligthly flattened with $q_H \sim 0.8$. Polar orbits are significantly underpopulated.

As it can be seen in Fig. A1, the final density profile is rather well described by an isothermal spheroid

$$\rho(R,\, z) = \frac{\tilde{\rho}_{\circ H}}{R^2 + z^2/q_H^2} \tag{A.1}$$

with $q_H \simeq 0.8$. An anisotropy in the disk plane is not seen, which is not surprising due to the model assumptions. The density profile is slightly dimpled at the poles which again is a consequence of the LMC and SMC orbits. The radially integrated MACHO-density decreases towards the poles and falls below $80\%$ of its average value at a galactic latitude higher than $\simeq 70$ degrees. Although the MACHO-density also varies azimuthally by about $10\%$, a clear correlation or anti-correlation with the final position of the LMC or SMC is not seen.

The angular dependence of the optical density $\tau$ is quite similar to the radially integrated MACHO-density. Due to the geometrical factor when integrating along the line of sight, the variation is somewhat weaker. In fact, the simulation implies that the optical density towards the LMC should not differ more than $\sim 20\%$ from the average value as a consequence of the halo flattening induced by the presence of the LMC and SMC.

Contrary to the density profile the velocity dispersion of the halo objects significantly varies with its position in the halo. Hence, the global distribution function in phase-space cannot be written as a product of a spatial and a velocity distribution. In fact, close to the LMC we even observe a bulk motion of MACHOs which form a separate halo around the LMC. Towards an undisturbed direction far from the LMC or the SMC, the velocity distribution is rather well described by a Maxwell

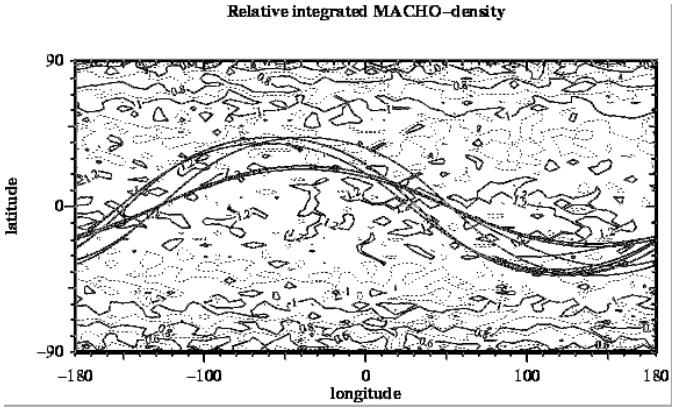


**Fig. A.2.** Relative integrated MACHO-density $\rho$ for an observer in the center of the halo. The distance to the source is set to be $50$ kpc. The trajectories show the projected orbits of the two massive companions. At the end of the simulation the LMC is located at $l = 80.7$, $b =$-31.3 and the SMC at $l = 93.7$, $b =$-30.4.

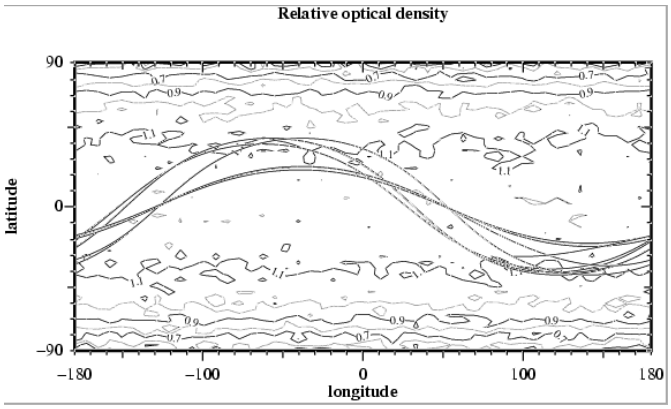


**Fig. A.3.** Relative optical density $\tau$ for an observer in the center of the halo. The distance to the source is set to be $50$ kpc. The trajectories show the projected orbits of the two massive companions. At the end of the simulation the LMC is located at $l = 80.7$, $b =$-31.3 and the SMC at $l = 93.7$, $b =$-30.4.

distribution with a dispersion velocity depending on the observational position.

For various locations in the halo the tangential velocity dispersion $v_H$ as given by the simulation is tabulated in Table 3. To calculate the tangential velocity dispersion, as used in gravitational microlensing from the simulated spatial one, we use

$$v_H^2 = \sqrt{(v_y v_z \cos\varphi \sin\vartheta)^2 + (v_x v_z \sin\varphi \sin\vartheta)^2 + (v_x v_y \cos\vartheta)^2}\,, \tag{A.2}$$

where $\varphi$ and $\vartheta$ denote the azimuthal and the declination angle of the observational direction in standard spherical coordinates.

## References

Alard C., 1997, A&A **321**, 424

Alard C., Guibert J., 1997, A&A **326**, 1
Alcock C. et al., 1993, Nature **365**, 621
Alcock C. et al., 1997a, ApJ. **479**, 119
Alcock C. et al., 1997b, ApJ. **486**, 697
Alcock C. et al., 1997c, ApJ **491**, L11
Ansari R. et al., 1999, A&A **344**, L49
Auburg E. et al., 1993, Nat **365**, 623
Bahcall J.N., Schmidt M., Soneira R.M., 1983, ApJ **265**, 730
Bahcall N.A., 1997, Dark Matter. In: Turok, N. (ed.) Critical Dialogues in Cosmology. World Scientific, Singapore, p. 221
Baillon P. et al., 1993, A&A **277**, 1
Binney J., Tremaine S., *Galactic Dynamics*, (Princeton University Press, 1987)
Crotts A.P.S., 1992, ApJ **399**, L43
Crotts A.P.S., Tomaney A.B., 1996, ApJ **473**, L87
De Paolis F., Ingrosso G., Jetzer Ph., 1996, ApJ **470**, 493
Derue F. et al., 1999, astro-ph 9903209
De Rújula A., Jetzer Ph., Másso E., 1991, MNRAS **250**, 348
De Rújula A., Jetzer Ph., Másso E., 1992, A&A **254**, 99
Dwek E. et al., 1995, ApJ **445**, 716
Freudenreich H.T., 1998, ApJ **492**, 495
Gates E.I., Gyuk G., Turner M.S., 1995, Phys. Rev. Lett. **74**, 3724
Gilmore G., Wyse R.F.G., Kuijken K., 1989, ARA&A **27**, 555
Griest K., 1991, ApJ **366**, 412
Griest K. et al., 1991 **84**, 752
Gyuk G., Holder G.P., 1998, MNRAS **297**, L44
Gyuk G., Dalal N., Griest K., 1999, astro-ph 9907338
Han C., Gould A., 1995, ApJ **447**, 53
Han C., 1997, ApJ **484**, 555
Holder G.P. and Widrow L.M., 1996, ApJ **473**, 828
Jetzer Ph., 1994, ApJ **432**, L43
Jetzer Ph., 1996, Helv. Phys. Acta **69**, 179
Jetzer Ph., Strässle M., Wandeler U., 1998, A&A **336**, 411
Kiraga M., Paczyński B., 1994, ApJ **430**, L101
Kochanek C.S., 1996, ApJ **457**, 228
Lin D.N.C., Jones B.F., Klemola A.R., 1995, ApJ **439**, 652
Mansoux B., 1997, PhD Thesis, LAL report 97-19
Paczyński B., 1986, ApJ **304**, 1
Paczyński B. 1991, ApJ **371**, L63
Palanque-Delabrouille N. et al., 1998, A&A **332**, 1
Peale S.J. 1998, ApJ **509**, 177
Peale S.J. 1999, astro-ph/9908154
Perdereau O., 1998, astro-ph/9812045
Reid N.I. et al., 1999, ApJ **521**, 613
Rhoads J.E., Malhotra S., 1998, ApJ **495**, L55
Salati P. et al., 1999, astro-ph/9904400
Udalsky A. et al., 1994, Acta Astronomica **44**, 165
Udalsky A. et al., 1997, Acta Astronomica **47**, 319
Westerlund B.E., 1990, A&A Rev **2**, 29
Zhao H.S., Spergel D.N., Rich R.M., 1995, ApJ **440**, L13